

Numerical study on a bubble dynamic generated by ultrasound waves in liquid-saturated porous media

F. Rambarzin*, M. T. Shervani-Tabar**, M. Taeibi-Rahni***

*Department of Mechanical and Aerospace Engineering, Science and Research branch, Islamic Azad University, Tehran, Iran, E-mail: f.rambarzin@sbiau.ac.ir

**Department of Mechanical Engineering, University of Tabriz, Tabriz, Iran, E-mail: msherv@tabrizu.ac.ir

***Department of Mechanical and Aerospace Engineering, Science and Research branch, Islamic Azad University, Tehran, Iran, E-mail: taeibi@sharif.edu

crossref <http://dx.doi.org/10.5755/j01.mech.22.6.17275>

1. Introduction

Due to the applications and important roles of cavitation bubbles in various industries and medicine, many researches has been carried out on the bubble dynamics in the vicinity of various surfaces and in a confined spaces. These studies show that the bubble behavior is highly dependent on its neighbor boundary. The applications role of the bubbles in a confined space can be mentioned in medicine [1], and also it can be used in food industry for processing [2], with the assistance of ultrasound waves. The main intention of this study is recognition of the role of bubbles in governing mechanism of the enhancing oil recovery assisted ultrasound waves (EOR/US). The growth and collapse of the vapor bubbles are the outcome of the transferred energy to the porous medium via the ultrasonic waves. The growth and collapse of the vapor bubble and the liquid jet formation cause a highly explosive movement in the fluid in the cavities of the porous media. The liquid movement in the cavities of a porous medium increases the permeability, and leads to enhancing oil recovery. Many laboratory observations shows the increasing of the enhanced oil recovery, using ultrasound waves. Duhon [3] was one of the first researchers who tested ultrasound waves radiation on the oil-saturated sandstone and observed increasing oil recovery. He has explained that the reason of the enhanced oil recovery is formation of the cavitation bubbles because of the transmitted energy of the ultrasound waves that causes a force on the trapped oil drops inside the pores and increases the permeability. Gadiev [4] radiated the ultrasound waves with a frequency of 15-40 kHz to the oil-saturated sandstone, and he observed a significant increase in the rate of oil recovery and explained its reason due to the Sono-Capillary Effect, and stated that the vapor bubbles formed by the ultrasound waves increase this effect.

Hamida and Babadagly [5] in their experimental research placed oil saturated sandstone in an ultrasound bath and observed that radiation of the ultrasound waves enhances oil recovery from the oil-saturated sandstone. Also, experimental observations of some researchers indicate increasing of the permeability of a porous medium and enhancing oil recovery by radiation of the ultrasound waves [6-9].

Rambarzin et al. [10] in their recent paper studied a cavitation bubble dynamics generated by the ultrasound waves in different types of pores of a porous medium numerically, to obtain the primary recognition of the govern-

ing mechanism of the increasing of the permeability of a porous medium via radiation of the ultrasound waves.

Finding the effect of increasing or decreasing the transferred energy to the porous medium is very important. Because it can be effective in identifying the limitations of the method and process optimization and energy saving methods. In this research, the effects of changes in the energy transmitted to the liquid-saturated cavity of a porous medium is investigated numerically. The problem is considered to be three-dimensional axisymmetric. In this paper, boundary element method (BEM) is employed for Numerical simulation of the problem under investigation.

2. Mathematical model

2.1. Assumptions and geometry of the problem

According to the physics of the problem, the cavity of the porous medium filled by brine. In the mathematical model, the liquid around the vapor bubble inside the cavity is assumed that an incompressible and inviscid, and the flow around the vapor bubble is irrotational. It is assumed that the scale bubble is in millimeters dimensions, so the effects of the buoyancy force can be ignored. The cavity surfaces of a porous medium are considered as rigid.

Geometry of the problem is shown in Fig. 1 that is the proposed model of the pores of a porous medium. In the middle of the liquid filled cavity is a small spherical vapor bubble. The vapor bubble grows symmetrically.

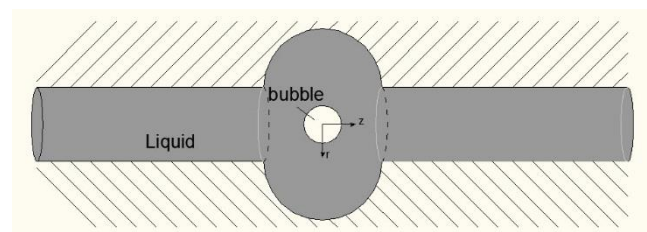


Fig. 1 Schematic representation of a cavity of a porous medium and a cavitation vapor bubble generated via ultrasound wave

2.2. Governing equations

It is assumed that the gases inside the cavitation vapor bubble are liquid vapor and non-condensable gas. Also it is assumed that the gas inside the vapor bubble satisfies the polytropic law with the polytropic exponent of γ ,

that γ is the special heat ratio inside the vapor bubble. Soh [11] and Soh and Shervani-Tabar [12] showed that if $\gamma = 1.15$, the numerical results will be more compatible with the experimental results of the cavitation bubbles behavior. In this study, the amount of γ is considered equal to 1.15. Through the balance of the forces exerted on the vapor bubble, it can be written as:

$$P(V) = P_c + P_0 \left(\frac{V_0}{V} \right)^\gamma - \sigma \kappa, \quad (1)$$

where $P(V)$ is the liquid pressure on the bubble surface which is equal to the pressure inside the bubble, P_c is saturated vapor pressure of the gas inside the bubble, P_0 is the initial gas pressure inside the bubble, V_0 is the initial volume of bubble and σ is the Surface tension of the liquid inside the cavity. In this study it is assumed that $\sigma = 0.0725 \frac{N}{m}$. κ is the average surface curvature. The average surface curvature for a Rotational symmetry axis surface, as Nitsche and steen [13] Calculated it, is given as below:

$$\kappa = \frac{1}{2} (\kappa_r + \kappa_z), \quad (2)$$

where κ_r and κ_z are principle radii of the curvatures, that can be defined as below:

$$\kappa_r = \frac{1}{r \left[1 + \left(\frac{dr}{dz} \right)^2 \right]^{\frac{1}{2}}}; \quad (3)$$

$$\kappa_z = - \frac{\frac{d^2 r}{dz^2}}{\left[1 + \left(\frac{dr}{dz} \right)^2 \right]^{\frac{3}{2}}}, \quad (4)$$

that r and z are radial axis and axis of symmetry respectively.

The equation that describes the motion of a spherical bubble in an infinite fluid domain, and is known as Rayleigh-Plesset equation and is given as [14]:

$$\left. \begin{aligned} R\ddot{R} + \frac{3}{2}\dot{R}^2 &= \frac{1}{\rho} \left[P_0 \left(\frac{R_0}{R} \right)^{3\gamma} - \frac{2\sigma}{R} - \Delta P \right]; \\ \Delta P &= P_\infty - P_c, \end{aligned} \right\} \quad (5)$$

where R is the radius of the bubble, \dot{R} and \ddot{R} are the first and second derivatives with respect to time, respectively that \dot{R} is the radial velocity and \ddot{R} is the radial acceleration of a spherical bubble. ΔP is the pressure difference between the pressure in the far field, P_∞ , and the vapor pressure inside the bubble, P_c .

The initial conditions for this problem are: $\dot{R} = 0$ at $R = R_0$, where R_0 is the initial bubble radius, and also

when the bubble reaches its maximum radius, $R = R_m$, $\dot{R} = 0$ occurs again. Before solving the problem, the Eq. (5) should be non-dimensionalized.

2.3. Non-dimensional equations

Non-dimensional parameters are defined as follows:

$$\left. \begin{aligned} \bar{r} &= \frac{r}{R_m}; \\ \bar{z} &= \frac{z}{R_m}; \\ \bar{R} &= \frac{R}{R_m}; \\ \bar{t} &= \frac{t}{R_m} \left(\frac{P_\infty - P_c}{\rho} \right)^{\frac{1}{2}}; \\ \bar{\phi} &= \frac{\phi}{R_m} \left(\frac{\rho}{P_\infty - P_c} \right)^{\frac{1}{2}}; \\ \varepsilon &= \frac{P_0}{\Delta P}; \\ \eta &= \frac{\sigma}{R_m \Delta P}, \end{aligned} \right\} \quad (6)$$

where the superscripts indicate the dimensionless parameters, ε is called the Strength parameter that can be considered as the amount of the transferred energy. η is the surface tension parameter, R is the radius of the bubble at any time, r is the radial axis, z is the axis of symmetry, ρ is the liquid density around the vapor bubble, and ϕ is the velocity potential.

Now, with analytical solution of the Eq. (5) and then making it dimensionless using the defined non-dimensional parameters and by satisfying the initial conditions, the Eq. (5) becomes as below [15]:

$$\frac{\varepsilon}{3-3\gamma} \left(\bar{R}_0^{-3\gamma} - \bar{R}_0^{-3} \right) + \frac{1}{3} \left(\bar{R}_0^{-3} - 1 \right) + \eta \left(\bar{R}_0^{-2} - 1 \right) = 0. \quad (7)$$

By solving the above equation in a given R_m , the maximum radius of the vapor bubble, and given ε and η , the initial dimensionless bubble radius, \bar{R}_0 , can be obtained by the Newton-Raphson method.

2.4. Boundary integral equation

According to the assumption of the potential fluid flow around the vapor bubble, the Green's integral equation is the governing equation for the fluid flow around the vapor bubble.

$$\left. \begin{aligned} 4\pi C_p \phi(p) + \int_s \phi(q) \frac{\partial}{\partial n} \left(\frac{1}{|p-q|} \right) ds &= \\ = \int_s \frac{\partial}{\partial n} \phi(q) \frac{1}{|p-q|} ds; \\ C_p &= 0.5 \text{ if } p \in S; C_p = 1 \text{ if } p \in \Omega, \end{aligned} \right\} \quad (8)$$

where s is the domain boundary including the vapor bubble surface, the cavity surface and the boundary at physical infinity; Ω is the liquid domain; p is any point in the liquid domain or on the boundary, and q is any point on the boundary.

2.5. Evaluating of time historical

The unsteady Bernoulli equation is employed for evaluating of time historical of the velocity potential and can be written as:

$$P_b = P_\infty - \rho \frac{\partial \Phi}{\partial t} - \frac{1}{2} \rho |\underline{u}|^2, \quad (9)$$

where P_b is the pressure inside the vapor bubble and \underline{u} is the mean velocity of the boundary of the vapor bubble.

3. Numerical computation

3.1. Discretization of the problem

Fig. 2 shows discretization of the boundaries of the suggested cavity model from a porous media.

The problem is considered axially symmetric. The cavity is saturated by liquid. The rigid surface of the cavity are discretized with linear elements and to avoid numerical instabilities, bubble boundary discretized by the cubic spline elements.

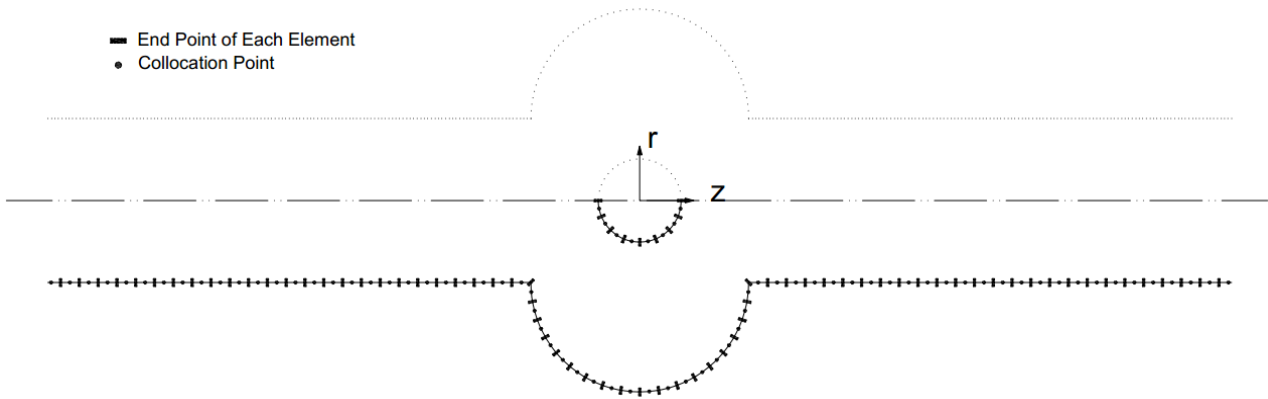


Fig. 2 Discretization of the boundaries of the proposed model of a cavity of a porous medium

Green integral equation that is mentioned in the Eq. (8), is discretized as follow:

$$\begin{aligned} C_{p_i} \phi(p_i) + \sum_{j=1}^m \int_{s_j} \phi(q_j) \frac{\partial}{\partial n} \frac{1}{|p_i - q_j|} ds = \\ = \sum_{j=1}^m \int_{s_j} \frac{\partial}{\partial n} \phi(q_j) \frac{1}{|p_i - q_j|} ds, \end{aligned} \quad (10)$$

Also discretized form of the unsteady Bernoulli equation with the Lagrangian approach is as follow:

$$\phi_j^{n+1} = \phi_j^n + \Delta t \left[\frac{P_\infty - P_b}{\rho} + \frac{1}{2} |\nabla \phi_j^n|^2 \right]. \quad (11)$$

Discretization of the rigid boundaries of the cavity continues to physical infinity. The collocation points are located in the middle of each element and the velocity potential and the normal velocity functions have been considered to be constant along each element.

3.2. Numerical procedure

The numerical calculations starts when the spherical vapor bubble via transmitted energy of the ultrasound waves into the liquid saturated cavity is in its initial minimum volume. The initial very high pressure inside the vapor bubble drives the bubble boundary, and the vapor bubble grows.

For obtaining the better numerical results, variable time step is obtained from the unsteady Bernoulli equation as follow:

$$\Delta t = \min \left| \frac{\Delta \phi}{\frac{P_\infty - P_b}{\rho} + \frac{1}{2} |\nabla \phi_j^n|^2} \right|, \quad (12)$$

where $\Delta \phi$ is an approximate constant number that indicates the maximum increase of the velocity potential on the vapor bubble boundary between the two consecutive time steps. At the beginning of the solution, the velocity potential on the bubble boundary and the normal velocity on the rigid surface given, and their value are equal to zero. With the given velocity potential at time t , by using the unsteady Bernoulli equation and fourth-order Runge-Kutta method, the velocity potential on the bubble boundary for the next time step, $t + \Delta t$, can be obtained.

4. Numerical results and discussion

Fig. 3 shows the evolution of the cavitation vapor bubble which is generated by the transmitted energy of the ultrasound waves to a liquid-saturated cavity. In the vapor bubble growth phase, as seen in the Figs. 1-3, the vapor bubble expands along the axis of symmetry. Then the liquid particles in the vicinity of the vapor bubble are accelerated away from the vapor bubble to the left and right sides. The accelerated liquid particles apply impact forces on possible obstacles in the left and right sides of the cavity. The applied forces could lead to removing of the possible obstacles, i.e. clays or sands, and consequently the permeability of the porous medium increases.

At the end of the growth phase, two high pressure range are created on the both sides of the vapor bubble. Due to the pressure difference created between this high pressure region and the pressure inside the vapor bubble, liquid jet develops around the vapor bubble and it takes the shape of an hourglass. This stage is called the necking phenomenon.

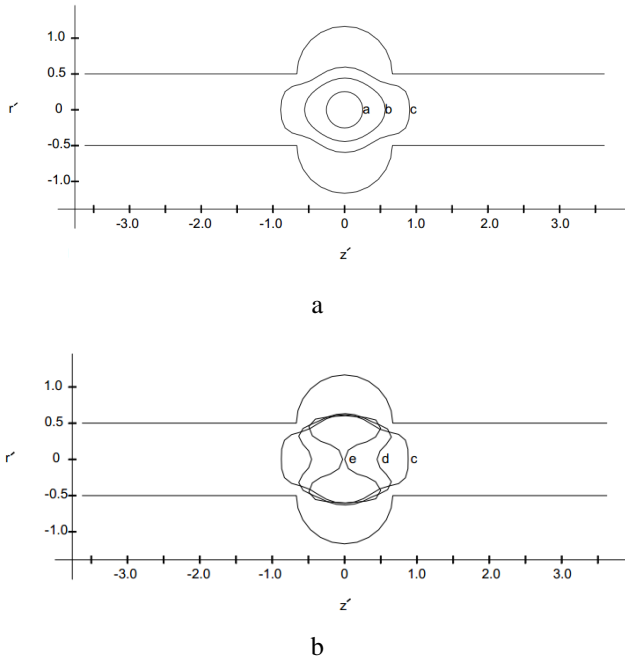


Fig. 3 Bubble's evolution in the center of the cavity of a porous medium with profiles: a - a-c: growth phase; b - c-e: collapse phase

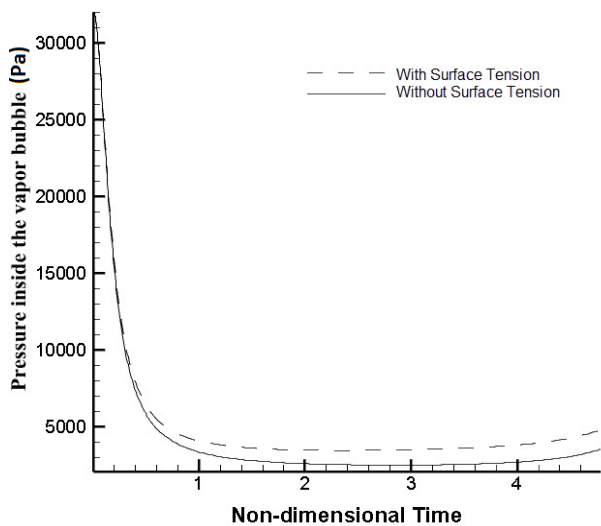


Fig. 4 Time history of the pressure inside the vapor bubble

Fig. 4 illustrates the changes of the pressure inside the vapor bubble with respect to the non-dimensional time during the growth and collapse phases in the cases of with and without the surface tension. As it is clear in figure 4, in the case of existence of the surface tension, during the growth phase of the vapor bubble, due to the inertia the vapor bubble can not grow enough than the case of without surface tension. So the pressure drop rate inside the vapor bubble is higher for the case of without surface tension. Fig. 5 shows time history of the variations of the non-dimensional liquid jet velocity on both sides of the vapor

bubble. As it can be seen in this figure, during the growth and collapse phases of the vapor bubble in the cases of with and without surface tension, the two diagrams almost overlap each other. Given the scale of the problem which is millimeter, the effect of the surface tension on the liquid jet velocity is negligible.

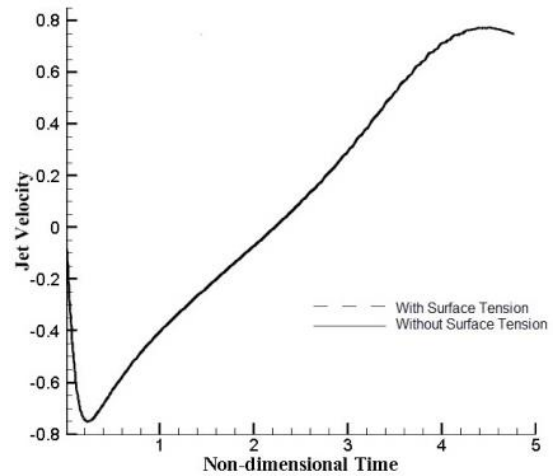


Fig. 5 Variations of liquid jet velocity, at both sides of the bubble the non-dimensional time during the phases of growth and collapse for the cases: with surface tension and without surface tension

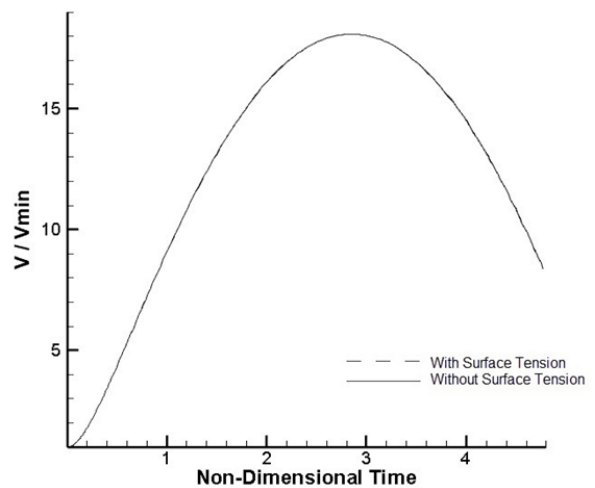


Fig. 6 Time history of the variation of the relative volume of the vapor bubble during its growth and collapse phases for the cases: with and without surface tension

Fig. 6 shows the rate of the growth and collapse phases of the vapor bubble in two cases: with surface tension and without surface tension. As it has been illustrated two graphs are overlap. However, to see the effects of surface tension, charts at the end of growth and collapse phases with higher precision drawn in Figs. 7, a and b. Because this result could be useful for micro scale of the problem that surface tension is important. As it has been shown in Figs. 7, a and b, the rate of the growth and collapse phases of the vapor bubble in the case of existence surface tension is lower than the case of without surface tension. It can be concluded from Fig. 7, b that the bubble lifetime in the condition of the presence the surface tension compared to the case of the absence surface tension is higher.

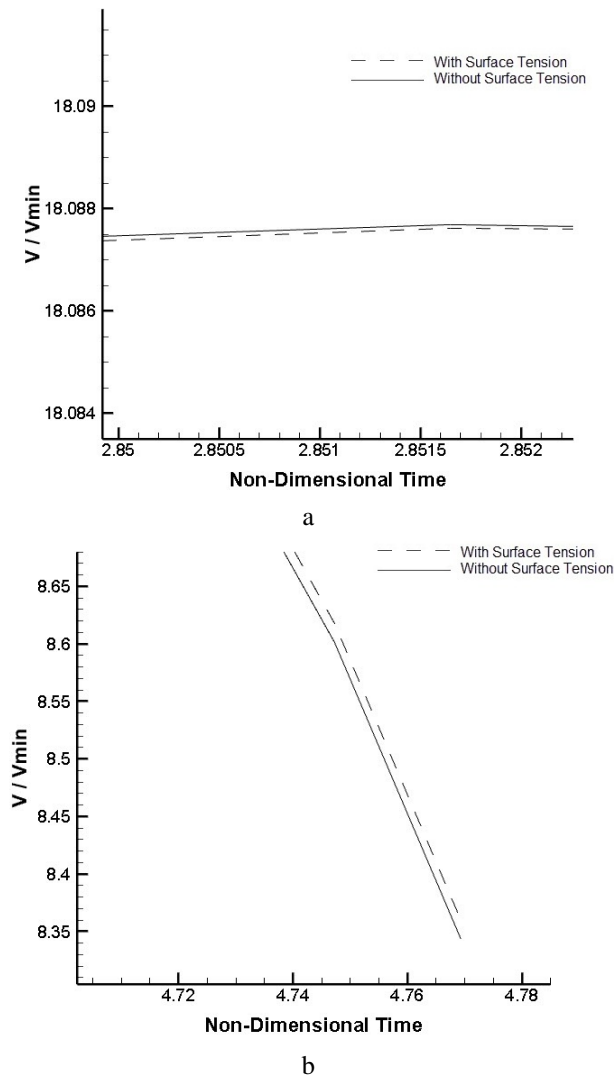


Fig. 7 Magnified time history of the variation of the relative volume of the vapor bubble for the cases with and without surface tension in: a - end of the growth phase; b - end of the collapse phase

To investigate the effects of the transmitted energy to a liquid-saturated porous medium, the transferred energy is increased 2.5, 5 and 10 times. It should be considered that the energy intensity of the ultrasound waves can not be increased indefinitely, because the maximum size of the bubbles is also dependent on the pressure amplitude, because may be not sufficient time for collapsing of the vapor bubble in a wavelength.

Fig. 8 illustrates rate of the growth and collapse phases of the bubble in the different amount of the transmitted energy to the liquid-saturated cavity of a porous medium. As it can be seen in the diagram, with the increase in the energy intensity that specified by the arrow in the figure, the rate of the growth and collapse phases of the vapor bubble shows significant increase, but there were no significant changes in lifetime of the vapor bubble.

Fig. 9 shows the variation of liquid jet velocity on both sides of the vapor bubble that are developed during the collapse process of the vapor bubble in different transmitted energy intensities. As can be seen in this figure, by reducing the energy intensity has been transferred that shown by the arrow in Fig. 9, in the both sides of the vapor bubble, the liquid particles along the axis of symmetry are less acceleration.

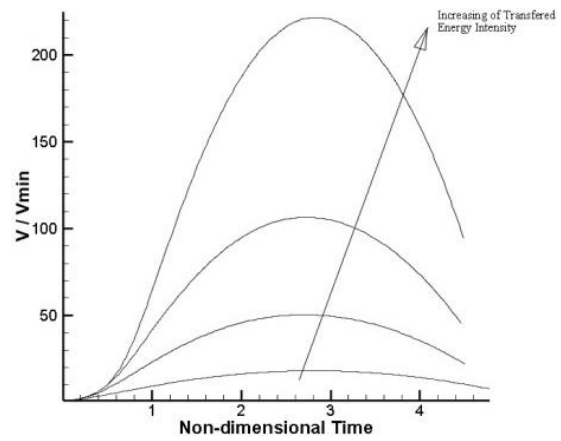


Fig. 8 Variations of the bubble volume relative to the minimum volume in non-dimensional time, during the process of growth and collapse with different intensities of transmitted energy to the liquid-saturated cavity of a porous medium

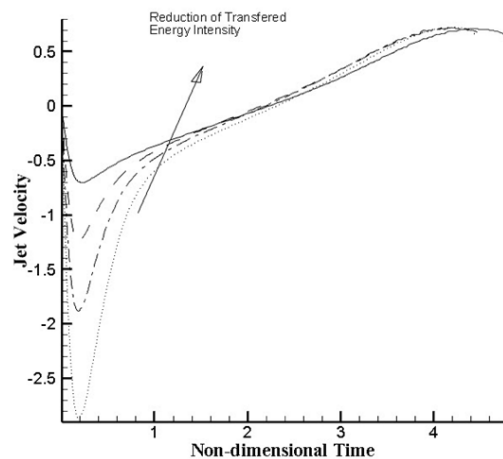


Fig. 9 Variations of liquid jet velocity on both sides of the bubble along the axis of symmetry relative to non-dimensional time for different transmitted energy intensity

5. Conclusion

In this paper, the dynamics of cavitation bubbles with different energy transfer and in the presence and absence of surface tension, the pores of the porous medium saturated with a liquid such as oil wells was studied numerically. With the increase in energy intensity has been transferred to a fluid-filled canal in a porous medium speed growth and decay phase shows a significant increase. But not observed significant changes in longevity bubble. The fluid particles through porous media on both sides of bubbles along the axis of the model are accelerated by increasing the intensity of transmitted energy. As a result, the force applied to the possible barriers at both ends of the cavity increases which ultimately increases the permeability of the porous medium. Increasing the permeability of the oil wells will result in increased oil recovery. The results show that the effect of surface tension on the results is not significant because of the scale of the problem. But to extend it to issues that porous medium filled with fluids with different surface tension and the problem is a micro scale dimension, on closer examination showed that surface tension is applied in the problem, because of the inertia of the growth of bubbles, the bubbles can not grow as

much as the absence of surface tension is not applied, Because of the inertia of the bubble growth, Bubbles could not grow enough when the surface tension is not applied, therefore in absence of surface tension is greater pressure drop rate inside the vapor bubble. The numerical results also showed that if the surface tension to be applied in the problem, collapsing of the vapor bubble later than when the surface tension is not considered. Results show that the rate of growth and collapse phases of the vapor bubble in the case of existence surface tension is less than the case of absence surface tension.

References

1. **Brennen, C.E.** 1995. *Cavitation and Bubble Dynamics*, Oxford University Press, 254p.
2. **Chemat, F.; Huma, Z.; Khan, M.K.** 2011. Applications of ultrasound in food technology: Processing, preservation and extraction, *Ultrasonics Sonochemistry* 18: 813-835.
<http://dx.doi.org/10.1016/j.ultsonch.2010.11.023>.
3. **Duhon, R.D., Campbell, J.M.** 1965. The effect of ultrasonic energy on flow through porous media, 2nd Annual Eastern Regional Meeting of SPE/AIME, Society of Petroleum Engineers, SPE 1316 WV.
<http://dx.doi.org/10.2118/1316-MS>.
4. **Gadiev, S.M.** 1977. *Use of Vibrations in Oil Production*, Moscow, Nedra Press.
5. **Hamida, T.; Babadagli, T.** 2007. Analysis of capillary interaction and oil recovery under ultrasonic waves, *Transp. Porous Med.* 70: 231-255.
<http://dx.doi.org/10.1007/s11242-006-9097-9>.
6. **Fairbanks, H.V.; Chen, W.I.** 1971. Ultrasonic acceleration of liquid flow through porous media, In *AICHE Symp. Ser.* 67: 105 (United States).
7. **Wong, S.-W.; van der Bas, F.; Zuidervijk, P.; Birchak, B.; Han, W.; Yoo, K.; Van-Batenburg, D.** 2003. High power/high frequency acoustic stimulation - a novel and effective wellbore stimulation technology, Society of Petroleum Engineers.
<http://dx.doi.org/10.2118/84118-MS>.
8. **Beresnev, I.A.; Johnson, P.A.** 1994. Elastic-wave stimulation of oil production-a review of methods and results, *Geophysics* 59(6): 1000-1017.
<http://dx.doi.org/10.1190/1.1443645>.
9. **Abramova, A.; Abramov, V.; Bayazitov, V.; Gerasin, A.; Pashin, D.** 2014. Ultrasonic technology for enhanced oil recovery, *Engineering* 6: 177-184.
<http://dx.doi.org/10.4236/eng.2014.64021>.
10. **Rambarzin, F.; Shervani-Tabar, M.T.; Taeibi-Rahni, M.; Tabatabaei-Nejad, S.A.** 2016. Energy transfer in a liquid filled elemental passage of a porous medium for permeability enhancement due to pulsations of a vapor bubble, *Mechanika* 22(1): 25-30.
<http://dx.doi.org/10.5755/j01.mech.22.1.14238>.
11. **Soh, W.K.** 1992. An energy approach to cavitation bubbles near compliant surfaces, *App. Math. Modeling* 10: 263-268.
[http://dx.doi.org/10.1016/0307-904X\(92\)90018-X](http://dx.doi.org/10.1016/0307-904X(92)90018-X).
12. **Shervani-Tabar, M.T.** 1995. Computer study of a cavity bubble near a rigid boundary, a free surface, and a compliant wall, Doctor of Philosophy thesis, Department of Mechanical Engineering, University of Wollongong.
<http://ro.uow.edu.au/theses/1576>.
13. **Nitsche, M.; Steen, P.H.** 2004. Numerical simulations of inviscid capillary pinchoff, *Journal of Computational Physics* 200: 299-324.
<http://dx.doi.org/10.1016/j.jcp.2004.04.005>.
14. **Plesset, M.S.** 1949. The dynamics of cavitation bubbles, *App. Mech.* 16: 228-231.
15. **Ni, B.Y.; Zhang, A.M.; Wang, Q.X.; Wang, B.** 2012. Experimental and numerical study on the growth and collapse of a bubble in a narrow tube, *Acta Mechanica Sinica* 28(5): 1248-1260.
<http://dx.doi.org/10.1007/s10409-012-0147-y>.

F. Rambarzin, M. T. Shervani-Tabar, M. Taeibi-Rahni

NUMERICAL STUDY ON A BUBBLE DYNAMIC GENERATED BY ULTRASOUND WAVES IN LIQUID-SATURATED POROUS MEDIA

S u m m a r y

In this paper, the effect of increasing or decreasing energy transferred by ultrasound waves on the dynamics of a cavitation vapor bubble in a confined space such as pores of a porous medium saturated liquid is investigated. The main motivation of this investigation is identifying and understanding the mechanisms of the enhanced oil recovery using ultrasound waves method in order to be able to recognize the limitations and important parameters in this method. Boundary element method for the numerical solution is used. The problem is solved for the cases with and without surface tension. Numerical results show that by increasing the amount of energy transferred to the liquid filled cavity, bubble growth and collapse rates shows a significant increase which results the acceleration of liquid particles around the vapor bubble at both ends of the cavity. As a result, the exerted force on the possible obstacles, like sand particles or trapped oil droplets, increases and moves them. Consequently the permeability of the porous medium increases. Increasing the permeability of oil well, leads to Enhanced Oil Recovery. The numerical results show that with increasing energy transferred to saturated liquid cavity, no significant changes occurs during the life time of the vapor bubble. The results also show that the effect of surface tension on the results, given the scale of the problem, is not significant.

Keywords: porous medium, permeability, ultrasound waves, vapor bubble, energy, boundary element method (BEM).

Received July 21, 2016

Accepted November 25, 2016